EPJ Web of Conferences **109**, 05002 (2016)
DOI: 10.1051/epjconf/201610905002

Neutrino-induced Reactions and Neutrino Scattering with Nuclear Targets

Myung-Ki Cheoun[1,a], Eunja Ha[1], Ghil-Seok Yang[1], Kyungsik Kim[2], and T. Kajino[3]

[1] *Dept. of Physics, Soongsil Univ., Seoul 156-743, Korea*
[2] *School of Liberal Arts and Science, Korea Aerospace University, Goyang 412-791, Korea*
[3] *National Astronomical Observatory of Japan, Tokyo 181-8588, Japan and Department of Astronomy, Graduate School of Science, University of Tokyo, Hongo 7-3-1, Bunkyo-ku, Tokyo 113-0033, Japan*

Abstract. We reviewed present status regarding experimental data and theoretical approaches for neutrino-induced reactions and neutrino scattering. With a short introduction of relevant data, our recent calculations by distorted-wave Born approximation for quasielastic region are presented for MiniBooNE data. For much higher energy neutrino data, such as NOMAD data, elementary process approach was shown to be useful instead of using complicated nuclear models. But, in the low energy region, detailed nuclear structure model, such as QRPA and shell model, turn out to be inescapable to explain the reaction data. Finally, we discussed that one step-process in the reaction is comparable to the two-step process, which has been usually used in the neutrino-nucleosynthesis.

1 Introduction

The neutrino (ν) is one of the most elusive particles in modern physics. But, nowadays many sources of the neutrino are known and available in the laboratory, whose energy range are located from a few MeV to a few TeV region [1]. In this paper, we mainly focus on the neutrino produced in the accelerator, in particular, LSND [2], MiniBooNE [3, 4] and NOMAD [5] data. The accelerator ν is emerging as a feasible probe for studying nuclear structures and related weak-interaction response, as well as various neutrino properties. Such ν-scattering can be applied to a wide variety of physics fields, such as astrophysics, cosmology, particle physics, and nuclear physics. For example, in nuclear physics, ν–nucleus (ν–A) scattering has become an essential tool for studying interesting weak-interaction physics, such as strangeness content in nucleons and matter distributions probed by Z^0 bosons which was also analyzed by parity-violating electron scattering [6, 7]. However, in the interpretation of the ν–A scattering data, the ambiguity stemming from the in-medium effect and the nuclear structure deserves to be examined in detail for further study of the weak interaction with nuclei or nuclear matter in other fields.

Since the first measurement of the muon-neutrino (ν_μ) scattering off a proton in a nuclear target via neutral current (NC) at the BNL [8], several ν-scattering experiments using NC and charged current (CC) have been performed at MiniBooNE, NOMAD [5] and MINERνA [9, 10]. These experiments mainly measured the flux-averaged CC and NC quasielastic (QE) cross sections on a nucleon inside a

[a] e-mail: cheoun@ssu.ac.kr

nuclear target composed by protons in C and Al, and CH_2 targets, respectively. In particular, the BNL NC data disclosed the strangeness contents on a nucleon, which was firstly discussed in Ref. [11].

Meanwhile, the MiniBooNE data addressed the fact that the experimental data are governed by the value of axial mass $M_A = 1.39 \sim 1.35$ GeV which is larger than the standard value $M_A = 1.03$ GeV and the strange axial form factor, *i.e.* $g_A^s = 0.08$ at $Q^2 = 0$, although there are many issues that remain unresolved [12]. One of these involves the in-medium effect due to the embedded nucleon in a nucleus. But the NOMAD data, which exploited high neutrino energy $E_\nu^{max} \sim 100$ GeV produced by the 450 GeV proton synchrotron (SPS, CERN), showed that the experimental data in the high energy region might be explained by $M_A = 1.05 \pm 0.02 \pm 0.06$ GeV [5].

Until now, many theoretical calculations [13, 14] for the MiniBooNE data have been reported in the viewpoint of nuclear physics. However, there are still several points to be discussed for further understanding the differences between theoretical results and the data as follows [12]: The first is multi-particle, multi-hole contributions beyond 1p–1h, which are found to be important for the CC reaction in the QE region [15]. The second is the ambiguity regarding a change in axial mass and strangeness content. The axial mass was increased about 30% to reproduce the CC and NC Mini-BooNE data with the strangeness content of the nucleon.

The third conjecture involves the neutrino flux evaluated from the simulation of pion production by proton scattering off a target and subsequent pion decays with neutrino emission. Recent data for the ν_μ and $\bar{\nu}_\mu$ disappearance at MiniBooNE and SciBooNE data [16, 17] provides grounds for a variety of new discussions, including the possibility of the sterile neutrino. The fourth possible contributions come from inelastic channels. More comprehensive coupled-channel approaches, including elastic and inelastic channels as well as two-nucleon knockout contributions, have yet to be developed. The last possibility is the explicit consideration of the in-medium effect by the modification of form factors embedded in the weak current [18, 19]. Our recent calculations [18, 19] by the distorted wave Born approximation (DWBA) and the quasi-particle random phase approximation (QRPA) [20] showed that differential cross sections for the neutrino-induced reaction in ^{12}C by an E_ν of less than 100 MeV may be altered by about $20 \sim 30$ % by the in-medium effect. In these calculations, we exploited the density-dependent weak form factors estimated in the quark-meson-coupling model (QMC) [21].

In the following, first we provide results by elementary process approach. Second, we present DWBA results. Finally, importance of the one-step process is discussed with the results by the QRPA calculation.

2 Elementary Process

Here we assume that $\nu(\bar{\nu})$ only interacts with nucleons inside a nucleus in the ν-A scattering. Then we exploit following cross section for $\nu(\bar{\nu})$ scattering off the nucleon inside target nucleus via NC (CC) by taking density-dependent form factors for the in-medium effects [22, 23]

$$\left(\frac{d\sigma}{dQ^2}\right)^{NC}_{\nu(\bar{\nu})} = \frac{G_F^2}{2\pi}\Big[\frac{1}{2}y^2(G_M^{NC})^2 + (1 - y - \frac{M}{2E_\nu}y) \tag{1}$$

$$\times\frac{(G_E^{NC})^2 + \frac{E_\nu}{2M}y(G_M^{NC})^2}{1 + \frac{E_\nu}{2M}y} + (\frac{1}{2}y^2 + 1 - y + \frac{M}{2E_\nu}y)(G_A^{NC})^2 \mp 2y(1 - \frac{1}{2}y)G_M^{NC}G_A^{NC}\Big]\,,$$

$$\left(\frac{d\sigma}{dQ^2}\right)^{CC}_{\nu(\bar{\nu})} = \left(\frac{d\sigma}{dQ^2}\right)^{NC}_{\nu(\bar{\nu})}(G_E^{NC} \to G_E^{CC}, G_M^{NC} \to G_M^{CC}, G_A^{NC} \to G_A^{CC})\,. \tag{2}$$

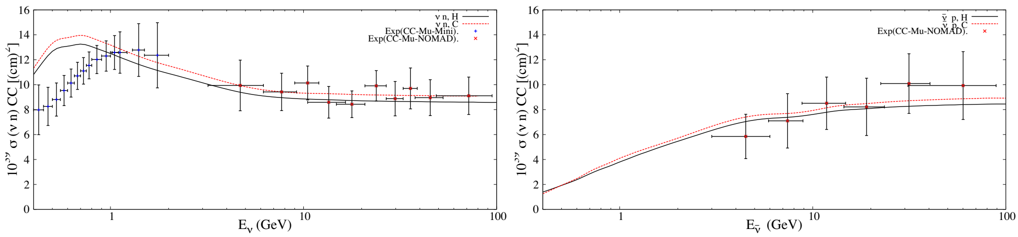

Figure 1. (Color online) Results of $\nu + n \rightarrow \mu^- + p$ (left) and $\bar{\nu} + p \rightarrow \mu^+ + n$ (right) for a nucleon in H and ^{12}C from Ref. [24]. Results for a free neutron (proton) and neutron (proton) in a carbon target are denoted as solid (black) and dotted (red) curves, respectively. Data are from Refs. [3, 5].

Here E_ν is the energy of the incident $\nu(\bar{\nu})$ in the laboratory frame, and $y = p \cdot q / p \cdot k = Q^2/2p \cdot k$ with k, p and $q(Q^2 = -q^2 \geq 0)$ as the respective initial four momenta of the $\nu(\bar{\nu})$ and target nucleon, and four momentum transfer to the nucleon. The sign, $-$ $(+)$, corresponds to ν $(\bar{\nu})$.

In Fig. 1, we compare the density-dependent elementary process to ν−A scattering cross section data from MiniBooNE CCQE events, where a CH_2 target is used and the data are plotted per neutron [3]. The in-medium effects, *i.e.* the difference of solid (black) and dotted (red) curves, turn out to be less than 3%. Nuclear effects, such as many-particle, many-hole configurations, final state interactions, and Coulomb distortion of outgoing leptons, need to be included for more realistic results. In particular, the Fermi motion of inside nucleons turns out to be important [14]. For example, our recent calculations using the distorted-wave Born approximation (DWBA) [12] show the importance of the nuclear effects and Coulomb distortion.

This trend is very similar to the Coulomb sum rule (CSR) calculation for inclusive QE electron scattering [25], which means that the overestimation should be suppressed by accounting for nuclear effects. Thus, our calculations indicate that in-medium effects cannot fully explain the MiniBooNE CCQE process; therefore, nuclear structure effects must be considered explicitly, as shown in our previous calculations [12].

However, in the very high energy region, the nuclear effects become small. We also compared our calculations to the NOMAD data [5] (red points in Fig. 1), where incident neutrino energy range goes to about 100 GeV. Total cross sections are described well by our elementary process and are shown to be nearly independent of the in-medium effects. For the higher energy region, we need to know a behavior of the form factors in high Q^2 region. Since all form factors are saturated in the high Q^2 region, in this paper, we used the saturated values for the high Q^2 region.

2.1 Neutral Current (NC) Scattering

For the MiniBooNE NC QE data, we treat the target as CH_2, which is composed of two free protons and the six neutrons and six protons of ^{12}C, in the following manner:

$$< \frac{d\sigma}{dQ^2} >= \frac{1}{7} < \frac{d\sigma_{\nu p \rightarrow \nu p, H}}{dQ^2} > + \frac{3}{7} < \frac{d\sigma_{\nu p \rightarrow \nu p, C}}{dQ^2} > + \frac{3}{7} < \frac{d\sigma_{\nu n \rightarrow \nu n, C}}{dQ^2} > , \tag{3}$$

where we took the efficiency-correction functions as unity. Results are shown in Fig. 2. By including the strangeness contents to NC scattering, the behavior in the low Q^2 region becomes in good agreement when including the strangeness contribution. However, the discrepancy in the high Q^2 region

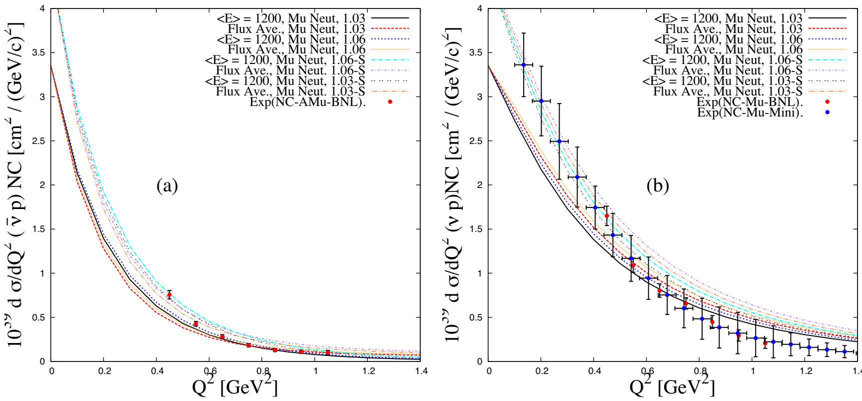

Figure 2. (Color Online) Flux-averaged and mean-averaged (E_ν = 1.2 GeV) differential cross sections from Ref. [24] for (a) $\bar{\nu}_\mu + p \to \bar{\nu}'_\mu + p$ and (b) $\nu_\mu + p \to \nu_\mu{}' + p$ scattering via NC, compared to the BNL [8] (left) and MiniBooNE data [4] (right). Theoretical results, which are calculated using averaged energy $< E > = 1.2$ GeV and by exploiting flux-averaged cross section $< d\sigma/dQ^2 >$, are given with (upper four curves) and without strangeness (lower four curves) for two different axial masses $M_A = 1.03$ and 1.06 MeV.

is still significant. Since we used the elementary process for ^{12}C, we thus take into account the in-medium effect in a finite nucleus by using density-dependent form factors. For ν–N in hydrogen, we use the elementary process with $\rho = 0$, but we use the density-dependent form factors at $\rho = 0.5\rho_o$ for ν–N in ^{12}C to account for in-medium effects. If we include the strangeness (upper four curves), results by $M_A = 1.03 \sim 1.05$ GeV are consistent with the data, regardless of the flux treatment in ν-A scattering.

The in-medium effects still cannot sufficiently explain the experimental–theoretical discrepancy, particularly in the high momentum-transfer region. The target effects that we included by the density dependence of nucleon form factors in the present calculations turn out not to be significant. Other nuclear structure effects and additional mechanisms, such as the final state interaction (FSI), are necessary for more comprehensive understanding [12]. Note that we do not use new values of the axial mass, M_A, and the axial strange form factor, g_A^s, obtained from the data [4], but instead exploit conventional values [19].

3 Distorted Wave Born Approximation (DWBA)

In the laboratory frame, the differential cross section for ν-A scattering in the QE region is given by the contraction between the lepton and the hadron tensors [18]

$$\frac{d\sigma}{dT_N} = 4\pi^2 \frac{M_N M_{A-1}}{(2\pi)^3 M_A} \int \sin\theta_l d\theta_l \int \sin\theta_N d\theta_N p f_{rec}^{-1} \sigma_M^Z [v_L R_L + v_T R_T + h v'_T R'_T], \tag{4}$$

where M_N is the nucleon mass, θ_l denotes the scattering angle of the lepton, and $h = -1$ ($h = +1$) corresponds to the helicity of the incident $\nu(\bar{\nu})$. θ_N and T_N represent the polar angle and the kinetic energy of the knocked-out nucleons, respectively. Detailed forms for the kinematical coefficients v, and the corresponding response functions R are given in our previous paper for $\nu - A$ scattering in Ref. [18]. In Eq. (4), the first term refers to the longitudinal, the second the transverse, and the last term the interference term.

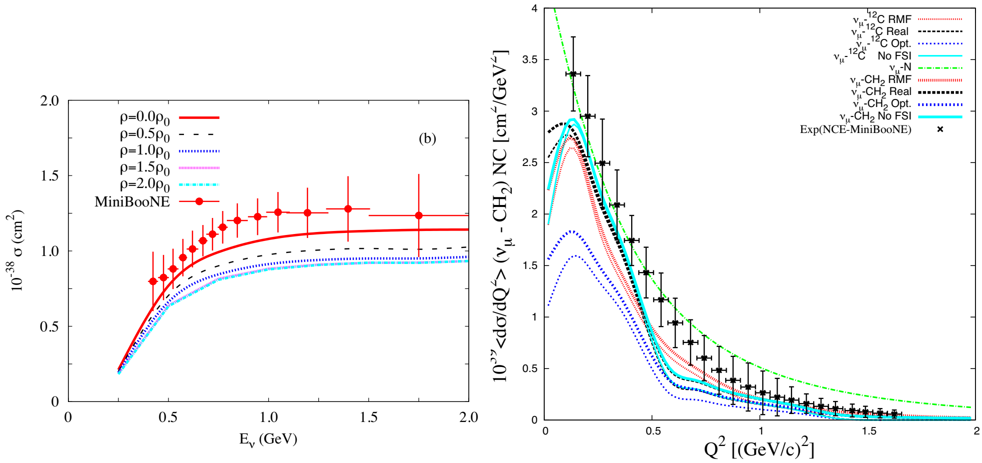

Figure 3. (Color online) Left panel from Ref. [12] is the total cross sections of the neutrino CC scattering in terms of the incident energies with $M_A = 1.39$ GeV. The experimental data are measured from MiniBooNE [21]. Right panel from Ref. [18] is flux averaged NC differential cross sections $< d\sigma/dQ^2 >$ per nucleon. Solid curve is the results for the No FSI, dotted curve is for the Optical, dashed curve is for the Real, and short-dotted curve is for the RMF. Thin curves are the results only for the ^{12}C target and thick curves are for the CH_2 target including the Hydrogen. The experimental data were measured from MiniBooNE experiment [9]. For a reference, results for ν-N are also presented in a green curve.

In the left panel of Fig. 3, we show the total cross sections of Eq. (4) for $^{12}\mathrm{C}(\nu_\mu, \mu)$ scattering in terms of the incident ν energies with the experimental data from MinBooNE [15]. We use the axial mass $M_A = 1.39$ GeV. The in-medium effects by the density dependent form factors [19] reduce the total cross sections by about 10 % for $\rho = 0.5\rho_0$, 15 % for $\rho = \rho_0$, 20 % for $\rho = 1.5\rho_0$, and 18 % for $\rho = 2.0\rho_0$. The red line, which is the DWBA calculation by the form factors in free space, is too small by about 40 %, if we use $M_A = 1.032$ MeV, by comparing with the experimental data. If we consider the nuclear density of ^{12}C as about 0.6 ρ_0, the discrepancy becomes about 60 % by comparing with the data. To reduce this discrepancy, we exploited the different value of the axial mass $M_A = 1.39$ GeV, but our results are still below the experimental data. Discussions on the final-state interaction by other approaches are summarized in the right panel and detailed in other papers [6, 12].

4 One-step process

By adopting the DWBA, we calculate ν-A scattering by assuming that incident $\nu(\bar{\nu})$ directly breakups nucleons in the target nucleus without any excitations. In Fig. 4, the cross sections of the one-step processes including the FSI are shown to be smaller than those by two-step process by a factor of 2 or 3 [26], although they depend on the optical potentials. Consequently, the contributions by the one-step processes to the relevant nuclear abundances are smaller by a factor 2 $\sim$ 4 than those by the two-step processes. If we recollect that the FSI of an outgoing nucleon is one of important ingredients on whole energy region, the relatively small contribution of the one-step process in Fig. 4 might be comparable to those of the two-step process if the FSI effects could be deliberately taken into account in the two-step process.

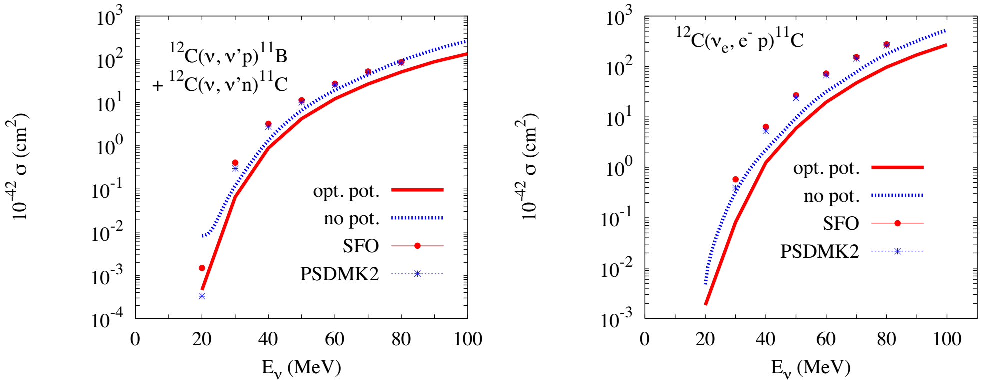

Figure 4. (Color Online) The NC and CC reaction by one-step processes, ^{12}C($\nu,\nu' p$)^{11}B + ^{12}C($\nu,\nu' n$)^{11}C , obtained by integrating the kinetic energy and summing all possible knocked-out nucleon states for ^{12}C($\nu,\nu' N$) reaction (see Ref. [26]). Data points for two-step processes, which are a sum of two cross sections, ^{12}C(ν,ν')$^{12}C^* \rightarrow ^{11}$B + p and ^{11}C +n, come from the shell model and the HF statistical calculation for a branching ratio into final states [2]. SFO and PSDMK2 mean two different Hamiltonians exploited in the calculation.

In summary, we applied the bound-nucleon weak form factors modified in a nuclear medium to ν and $\bar{\nu}$ QE scattering off a nucleon in dense matter or embedded in a finite nucleus, *i.e.* $\nu_\mu(\bar{\nu}_\mu)$ – N*. The form factors were calculated in the QMC model. We compared the density-dependent elementary-process results to recent experimental data performed at BNL, NOMAD and MiniBooNE, which used ^{12}C composite targets, by treating the wave functions of bound nucleons as plane waves modified by in-medium effects. Our method is efficient for understanding neutrino scattering data, but a more thorough approach incorporating nuclear structure is necessary for further discussions. Proper treatment of the Fermi motion of the bound nucleon is shown to be vital for the low $Q^2 < 0.2$(GeV/c)^2 region and low energy $E_\nu < 1$ GeV region. Additionally, the strangeness content of the nucleon turns out to be indispensable for interpreting NC scattering.

Secondly, in order to take the nuclear structure into account, we used the DWBA which has been successfully applied to electron scattering and explained most of MiniBooNE data. But M_A mass problem is still remained even if in-medium effects are taken into account. We also estimated, by using the DWBA, the possible one-step process coming from direct knockout of nucleons by incident neutrinos. The one-step process turned out to be not so small compared to the two-step process.

References

[1] https://icecube.wisc.edu/ (2015).
[2] L. B. Auerbach et al. (LSND Collaboration), Phys. Rev. C 64,065501 (2001).
[3] A. A. Aguilar-Arevalo *et al.* (MiniBooNE Collaboration), Phys. Rev. D **81**, 092005 (2010).
[4] A. A. Aguilar-Arevalo *et al.* (MiniBooNE Collaboration), Phys. Rev. D **82**, 092005 (2010).
[5] V. Lyubushkin *et al.* (NOMAD Collaboration), Eur. Phys. J. C **63**, 355 (2009).
[6] K. S. Kim and M. -K. Cheoun, J. of Phys. Soc. Japan **82**, 024201 (2013).
[7] O. Moreno, P. Sarriguren, E. Moya de Guerra *et al.*, Nucl. Phys. A **828**, 306 (2009).
[8] K. Abe *et al.*, Phys. Rev. Lett. **56**, 1107 (1986); L. A. Ahrens *et al.*, Phys. Rev. D **35**, 785 (1987).

[9] B. G. Tice *et al*. (MINERνA Collaboration), Phys. Rev. Lett. **112**, 231801 (2014).
[10] G. A. Fiorentini *et al*. (MINERνA Collaboration), Phys. Rev. Lett. **111**, 022502 (2013).
[11] W.M. Alberico *et al.*, Phys. Lett. B **438**, 9 (1998); Nucl. Phys. A **651**, 277 (1999).
[12] K. S. Kim, M. -K. Cheoun, W. Y. So, Phys. Rev. **C 88**, 044615 (2013)
[13] R. González-Jiménez, M. V. Ivanov, M. B. Barbaro *et al.*, Phys. Lett. B **718**, 1471 (2013).
[14] M. V. Ivanov, A.N. Antonov, J.A. Caballero *et al.*, Phys. Rev. C **89**, 014607 (2014).
[15] M. Martini, M. Ericson and G. Chanfray, Phys. Rev. **C 84**, 055502 (2011).
[16] K. B. M. Mahn *et al*. (MiniBooNE and SciBooNE Collabo.), Phys. Rev. **D 85**, 032007 (2012).
[17] G. Cheng *et al*. (MiniBooNE and SciBooNE Collabo.), Phys. Rev. **D 86**, 052009 (2012).
[18] K. S. Kim *et al.*, Phys. Rev. **C 90**, 017601 (2014); Phys. Rev. **C 91**, 014606 (2015).
[19] M. -K. Cheoun *et al.*, Phys. Rev. **C 87**, 065502 (2013); Phys. Lett. **B 723**, 464 (2013).
[20] M. -K. Cheoun *et al.*, J. Phys. G **37**, 055101 (2010); Phys. Rev. C. **81**, 028501 (2010).
[21] D. -H. Lu, K. Tsushima, A. W. Thomas, A. G. Williams and K. Saito, Phys. Rev. C **60**, 068201 (1999).
[22] M. -K. Cheoun and K. S. Kim, J. Phys. **G 35**, 065107 (2008).
[23] W. M. Alberico, S. M. Bilenky, C. Maieron, Phys. Rep. **358**, 227 (2002).
[24] M. -K. Cheoun *et al.*, J. Phys. G **42**, 045102 (2015).
[25] K. S. Kim, B. G. Yu and M. K. Cheoun, Phys. Rev. **C 74**, 067601 (2006).
[26] K. S. Kim, M.-K. Cheoun, Phys. Lett. B 679 330 (2009).